Available online at www.sciencedirect.com
SCIENCE DIRECT®
International Journal of Heat and Mass Transfer 48 (2005) 235–242
International Journal of HEAT and MASS TRANSFER
www.elsevier.com/locate/ijhmt

Convective boiling heat transfer characteristics of CO_2 in microchannels

Rin Yun [a], Yongchan Kim [a,*], Min Soo Kim [b]

[a] Department of Mechanical Engineering, Korea University, Anam-dong, Sungbuk-ku, Seoul 136-701, Korea
[b] Department of Mechanical and Aerospace Engineering, Seoul National University, Seoul 151-744, Korea

Received 25 June 2004; received in revised form 23 August 2004

Abstract

Convective boiling heat transfer coefficients and dryout phenomena of CO_2 are investigated in rectangular microchannels whose hydraulic diameters range from 1.08 to 1.54 mm. The tests are conducted by varying the mass flux of CO_2 from 200 to 400 kg/m^{2}s, heat flux from 10 to 20 kW/m^2, while maintaining saturation temperature at 0, 5 and 10 °C. Test results show that the average heat transfer coefficient of CO_2 is 53% higher than that of R134a. The effects of heat flux on the heat transfer coefficient are much significant than those of mass flux. As the mass flux increases, dryout becomes more pronounced. As the hydraulic diameter decreases from 1.54 to 1.27 mm and from 1.27 to 1.08 mm at a heat flux of 15 kW/m^2 and a mass flux of 300 kg/m^{2}s, the heat transfer coefficients increase by 5% and 31%, respectively. Based on the comparison of the data from the existing models with the present data, the Cooper model and the Gorenflo model yield relatively good predictions of the measured data with mean deviations between predicted and measured data of 21.7% and 21.2%, respectively.

Keywords: Microchannels; Microchannel heat exchanger; CO_2; Heat transfer coefficient; Boiling heat transfer

1. Introduction

A microchannel heat exchanger provides several advantages over a conventional fin-tube heat exchanger in a CO_2 transcritical system operating at high pressures. Microchannels can endure high operating pressure due to its channel structure. Besides, microchannels provide much larger contact area with fluid per unit volume and yield a higher heat transfer coefficient compared to that of a round tube. Although an additional contact area with the fluid increases the pressure drop in microchannels, CO_2 shows a relatively smaller pressure drop than other conventional refrigerants. With these advantages of microchannels, we can save space and material of a heat exchanger, and reduce its weight and refrigerant charge. However, the microchannel heat exchanger as an evaporator has the shortcomings of refrigerant maldistribution and condensed water drainage.

Since microchannel technology is relatively new, data on heat transfer coefficients are very limited in literature. Pettersen [1] studied flow vaporization of CO_2 in a microchannel tube with a diameter of 0.8 mm. He showed that dryout significantly affected heat transfer

* Corresponding author. Tel.: +82 2 3290 3366; fax: +82 2 921 5439.
E-mail address: yongckim@korea.ac.kr (Y. Kim).

0017-9310/$ - see front matter © 2004 Elsevier Ltd. All rights reserved.
doi:10.1016/j.ijheatmasstransfer.2004.08.019

Nomenclature

Bo	boiling number
D	diameter, m
G	mass flux, $kg\,m^{-2}\,s^{-1}$
H	heat transfer coefficient, $W\,m^{-2}\,K^{-1}$
k	thermal conductivity, $W\,m^{-1}\,K^{-1}$
M	molecular weight, $kg\,kmol^{-1}$
Pr	Prandtl number
p_r	reduced pressure
q	heat flux, $W\,m^{-2}$
R_p	surface roughness parameter, μm
Re	Reynolds number
T	temperature, K
We_l	Weber number based on liquid ($G^2D/\rho_l\sigma$)

Greek symbols

δ	film thickness, m
ϵ	void fraction
μ	dynamic viscosity coefficient, $N\,s\,m^{-2}$
ρ	density, $kg\,m^{-3}$
σ	surface tension, N/m

Subscripts

f	fluid
h	hydraulic
l	liquid
o	reference
v	vapor
w	inner wall

characteristics of CO_2 at high mass fluxes and high saturation temperatures, and nucleate boiling was dominant prior to dryout. Zhao et al. [2] presented experimental data for flow boiling of CO_2 and R134a in a microchannel for vapor qualities from 0.05 to 0.3. In their vapor quality range, mass flux had very small effect on heat transfer coefficients for both CO_2 and R134a. In addition, the heat transfer coefficient of CO_2 was approximately 200% higher than that of R134a. Hihara and Tanaka [3] reported boiling heat transfer coefficients of CO_2 in a 1.0 mm diameter single tube. They found that dryout of CO_2 depended on saturation temperature, mass flux, and heat flux. Yun et al. [4] investigated boiling heat transfer coefficients of CO_2 in mini tubes with inner diameters of 2.0 and 0.98 mm. The measured heat transfer coefficient was in the range of 10–20 kW/m^2K, which was significantly affected by dryout. The dryout generally occurred at vapor qualities from 0.3 to 0.4. Zhao et al. [5] developed heat transfer correlations for microchannels by modifying the Liu and Winterton correlation [6]. They used a confinement number to consider the effects of a small tube diameter.

The available literature on the subject of two-phase flow heat transfer in microchannels has not fully addressed the effects of microchannel size (hydraulic diameter) and operating parameters on heat transfer coefficients. Furthermore, heat transfer characteristics in multi-channels under dryout conditions should be investigated [7]. In this study, the boiling heat transfer coefficients in microchannels were measured and then analyzed as a function of mass flux, heat flux, and saturation temperature. The effects of hydraulic diameter and dryout on the heat transfer coefficients in microchannels were also studied. The measured heat transfer coefficients were compared with the predictions using the existing correlations for heat transfer coefficients in small diameter tubes.

2. Experimental setup and test conditions

Fig. 1 shows a schematic of the experimental setup. The test loop consists of a magnetic gear pump, a mass flow meter, a preheater, a test section, a control tank, and a condenser. The magnetic gear pump circulates the working fluid and the preheater adjusts the inlet vapor quality of the test section. Applying a direct current heating method, which uses a high-current transformer with 1000 A and 5 V, provided heat flux to the test section. The test section was heavily insulated using a rubber foam to minimize heat loss to the ambient. The heat loss was estimated by comparing the electric heat input with the actual heat transfer rate to CO_2 in terms of the enthalpy difference across the test section in subcooled state. The heat loss test was conducted at an average fluid temperature of 10 °C with the various heat and mass flux conditions. The heat loss in the preheater and test section was taken into account in the calculations of vapor quality and heat transfer coefficient by estimating the actual heat input to these sections based on the difference between the measured heat input and the heat loss.

The mass flow rate was measured using a Coriolis effect flow meter with an uncertainty of ±0.2% of reading. Wall temperatures of the test section and fluid temperatures were measured by T-type thermocouples with a calibrated accuracy of ±0.1 °C. Thermocouples were placed on the top and bottom of each measuring point, which were equally located along the test section. The junctions installed on the outer surface of the microchannels were electrically insulated by a very thin Teflon

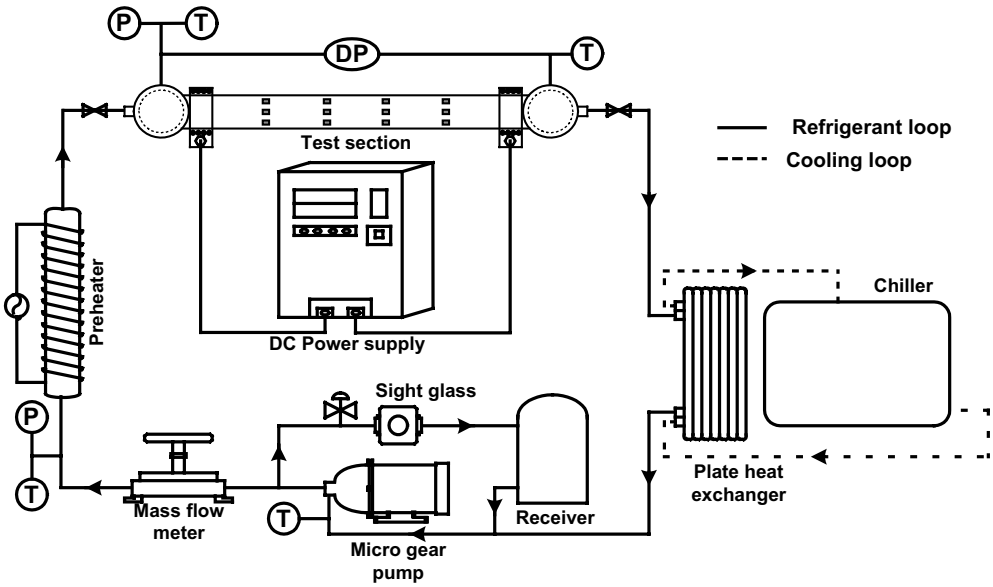

Fig. 1. Schematic of the experimental setup.

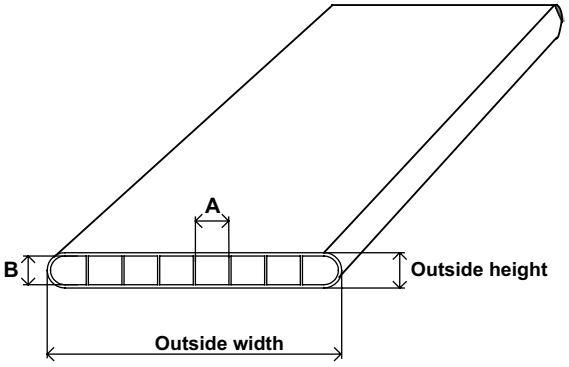

Fig. 2. Schematic of the test section.

tape. The temperature differences among the thermocouples during single-phase runs were less than ±0.2 °C. The pressure of the refrigerant entering the test section was monitored with a pressure transducer with an uncertainty of ±2.1 kPa. The power input to the preheater was monitored using a watt transducer with an uncertainty of ±0.2% on full scale.

The test microchannels have rectangular channels as shown in Fig. 2. Table 1 shows the specifications of five microchannels tested in this study. Hydraulic diameter of the test section varied from 1.08 to 1.54 mm. Fig. 3 shows the connecting parts of microchannels and the details of header. The height of the header was 120 mm and the hole was carefully machined to fit the microchannels. The tests were conducted at mass fluxes from 200 to 400 kg/m^{2}s, heat fluxes from 10 to 20 kW/m^2, and saturation temperatures from 0 to 10 °C.

The local heat transfer coefficient, h, was determined from the measured heat flux, q, the fluid temperature, T_f, and the calculated inner wall temperature, T_w.

$$h = q/(T_w - T_f) \tag{1}$$

The inner wall temperature, T_w, was calculated from the measured outer wall temperatures using the equations for steady state heat conduction through the microchannel and for heat generation within the wall. The heat flux was calculated from the ratio of power input to surface area in the microchannel.

Table 1
Specifications of the test tubes

Test tube no.	Outside width (mm)	Outside height (mm)	A (mm)	B (mm)	Number of channels	Hydraulic diameter (mm)
1	16	1.8	2.15	1.2	6	1.54
2	16	1.8	1.36	1.2	9	1.27
3	16	2.0	1.25	1.2	10	1.08
4	18	1.7	2.15	1.1	7	1.53
5	20	2.0	1.52	1.2	10	1.14

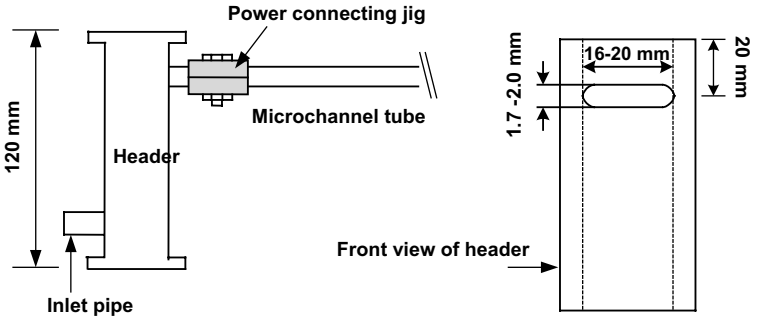

Fig. 3. Schematic of connecting parts and details of header.

Uncertainties of the present experiments were analyzed with the RRS method suggested by Maffat [8]. The average uncertainty was estimated by averaging the uncertainties calculated for each test condition, which were within 95% of reliability. In this study, the average uncertainty of the heat transfer coefficients was ±12.9%, which was calculated with an uncertainty of ±1.4% in the determination of the heat transfer rate to the test section. The average uncertainty of vapor quality at the inlet of the test section was ±4% calculated from the uncertainty of the enthalpy at the inlet of the test section.

3. Results and discussion

Fig. 4 shows the comparison of the present data with Pettersen et al.'s [1] for a microchannel. Both data show an existence of dryout at moderate vapor quality. After dryout, the heat transfer coefficient significantly drops due to an increase in tube wall temperature. The present data show similar trends with Pettersen et al.'s. However, the heat transfer coefficients reported by Pettersen et al. [1] show 19% higher values than the present data at the same heat flux. The possible reasons for higher heat transfer coefficient of Pettersen et al. are that their test channel had a smaller hydraulic diameter and they tested at a higher saturation temperature. Generally, the heat transfer coefficient of CO_2 increases with a rise of saturation temperature due to an enhancement of nucleate boiling.

Fig. 5 shows the influence of heat flux on boiling heat transfer coefficients for CO_2 and R134a. The heat transfer coefficient of CO_2 at a heat flux of 10 kW/m^2 increases with vapor quality, while it remains fairly constant at a heat flux of 15 kW/m^2. For a heat flux of 20 kW/m^2, the heat transfer coefficient of CO_2 is maintained constant up to a quality of 0.55, but it starts to decrease beyond that point. The rapid reduction of heat transfer coefficient at a certain quality is due to the dryout of the liquid film. As the heat flux increases, nucleate boiling becomes more active and bubble bursting near interface of the liquid film and vapor can occur more frequently. Especially, the liquid film of CO_2 breaks more easily from the tube wall due to a lower surface tension of CO_2, which causes an earlier dryout of the liquid film

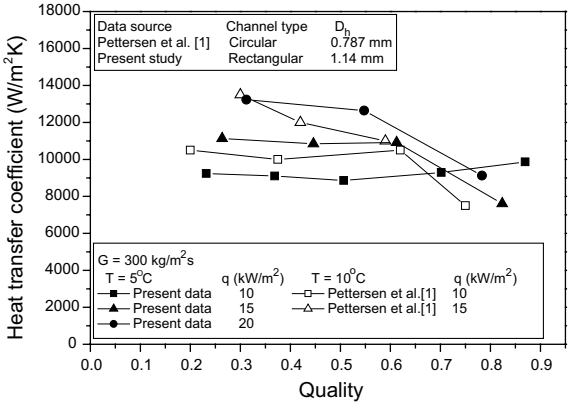

Fig. 4. Comparison of the present data with Pettersen et al.'s [1].

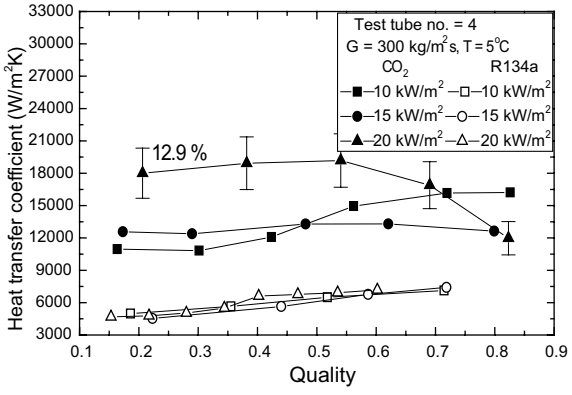

Fig. 5. Comparison of the heat transfer coefficients of CO_2 with those of R134a.

at a lower vapor quality. When the quality is less than 0.5, the boiling heat transfer coefficient of CO_2 increases with a rise of heat flux. However, when the quality is greater than 0.5, the effects of heat flux on the heat transfer coefficient of CO_2 become uncertain due to the dryout phenomenon. In case of R134a, the heat transfer coefficient increases with quality at all heat fluxes. The dryout quality of R134a is much higher than that of CO_2 due to a relatively higher surface tension of R134a. In addition, the effects of heat flux on the heat transfer coefficient of R134a are negligible as compared with those of CO_2. For a heat flux of 15 kW/m^2, the average heat transfer coefficient of CO_2 is 53% higher than that of R134a.

Fig. 6 shows the influence of saturation temperature on the heat transfer coefficients at a mass flux of 300 kg/m^{2}s and various heat flux conditions. The heat transfer coefficient increases with a rise of saturation temperature. The heat transfer coefficients at saturation temperatures of 5 and 10 °C increase by 13% and 30%, respectively, based on the data at a saturation temperature of 0 °C. Increasing saturation temperature can enhance nucleate boiling due to the decrease of surface tension. For example, the surface tensions of CO_2 at 0, 5, and 10 °C are 0.0046, 0.0036, and 0.0028 N/m, respectively. Moreover, as the heat flux increases from 10 to 15 kW/m^2 and 20 kW/m^2 at a saturation temperature of 5 °C, the heat transfer coefficients are improved by 18% and 38%, respectively. These enhancements can be attributed to an improvement of nucleate boiling heat transfer with the increase of heat flux.

Fig. 7(a) shows the effects of mass flux on the heat transfer coefficient when dryout occurs. When the mass flux is 200 kg/m^{2}s, the heat transfer coefficient remains nearly constant up to a quality of 0.8. However, as the mass flux increases from 200 to 300 kg/m^{2}s, a rapid reduction of the heat transfer coefficient is observed at a vapor quality of 0.7. The reduction of the heat transfer coefficient becomes more significant and the dryout quality decreases with a rise of mass flux. As the mass flux increases, the flow pattern transition to annular flow can occur easily [9] and the entrainment of liquid droplets into the vapor core becomes more active [10], which cause more pronounced dryout phenomenon. Fig. 7(b) shows the effects of mass flux on the heat transfer coefficient under non-dryout conditions. The effects of mass flux become negligible. This result is consistent with the test results reported by the previous studies [1,2]. In addition, the heat transfer coefficient varies relatively slightly with quality at all mass fluxes, which lies between 9000 and 11000 W/m^{2}K.

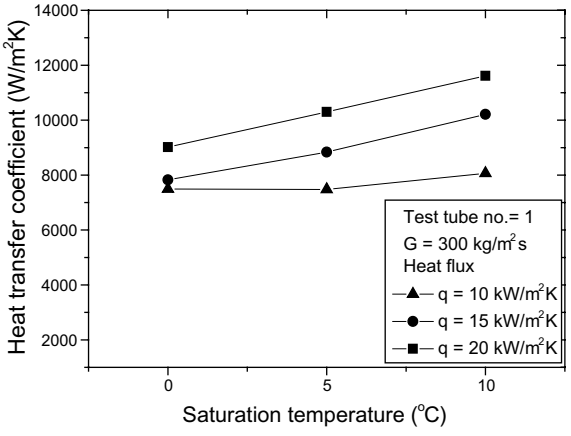

Fig. 6. Effects of saturation temperature.

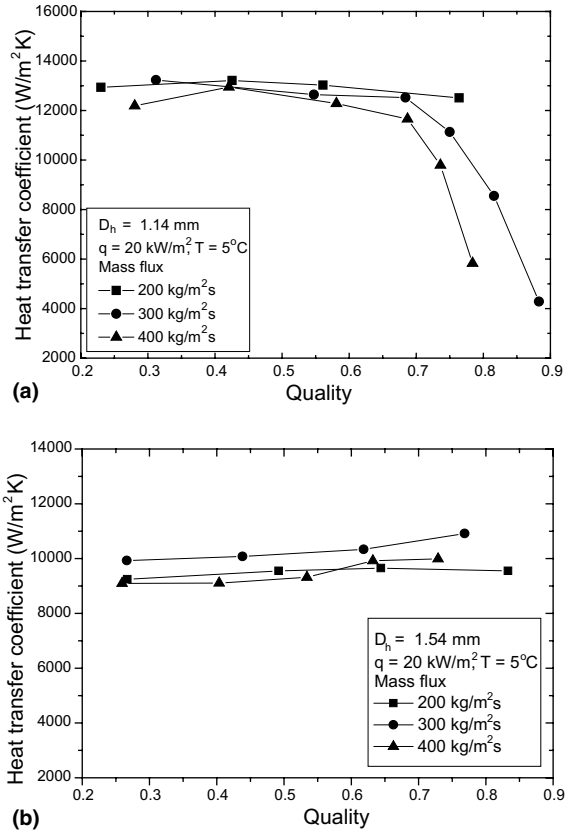

Fig. 7. Effects of mass flux on heat transfer coefficients. (a) Dryout conditions, (b) non-dryout conditions.

Fig. 8 shows the effects of hydraulic diameter on the average heat transfer coefficients. The heat transfer coefficient increases with the reduction of the hydraulic diameter at all heat fluxes. When the hydraulic diameter decreases from 1.54 to 1.27 mm and from 1.27 to 1.08 mm at a heat flux of 15 kW/m^2, the heat transfer coefficients increase by 5% and 31%, respectively. Reducing the hydraulic diameter of the microchannels tested in this study increases the perimeter, which makes

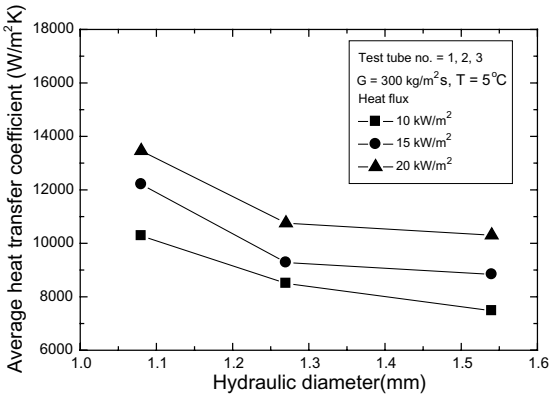

Fig. 8. Average heat transfer coefficients as a function of hydraulic diameter.

heat load distribution to each channel easier and effective. Also, it should be noted that nucleate boiling is much more dominant in microchannels with a smaller hydraulic diameter [11–13].

Table 2 shows the existing models developed for predicting convective boiling heat transfer coefficients in small diameter tubes. The present data are compared with the predictions made by the existing models and mean deviations are given in Table 2. The Cooper model [14] and the Gorenflo model [15], which were developed to predict nucleate boiling heat transfer coefficients, yield relatively good predictions of the present data with mean deviations of 21.7% and 21.2%, respectively. Since nucleate boiling is dominant in a small diameter tube and the surface tension of CO_2 is very small as compared to conventional refrigerants, these models show satisfactory predictions of the measured data. Although Lazarek and Black [16], and Tran et al. [17] used the term of *Bo* as a major parameter in their correlations, their models show large deviations from the present data. These large deviations may be attributed to the limitations of working fluids used in developing their models. The Liu and Winterton model [6] including a convective and a nucleate boiling term shows a close correlation with the measured data with a mean deviation of 25.6%. The Liu and Winterton model employed the Cooper model in the calculation of the nucleate boiling term. Kattan et al. [18] developed a model by considering the effects of annular flow pattern along with liquid film thickness and void fraction. This flow pattern is dominant in a small diameter tube. The Kattan et al. model [18] shows fairly consistent predictions of the present data with a mean deviation of 24.1%.

Fig. 9(a) and (b) show the comparison of the present data with the predictions using the existing models. Generally, all models considered in this study show large under-predictions at high heat transfer coefficients, which are above 15,000 kW/m^2K. These deviations may be due to the existence of a mal-distribution and large pressure fluctuation in multi-tubes, which yield the differences of heat transfer coefficients between microchannels and single tubes even though the tests were conducted at similar operating conditions. Therefore, further studies are required to develop a new heat transfer coefficient model that will include the flow instability of multi-channels to obtain better predictions.

4. Conclusions

In this study, the boiling heat transfer characteristics of CO_2 in microchannels were experimentally investigated by varying operating conditions and hydraulic diameter of microchannels. The average heat transfer coefficient of CO_2 was 53% higher than that of R134a. The effects of heat flux on the heat transfer coefficient

Table 2
Correlations used in predictions of heat transfer coefficients in microchannels

References	Correlation	Important parameters/comments	Mean dev. (%)[a]
Cooper [14]	$h = 55p_r^{0.12}(-\log_{10}p_r)^{-0.55}M^{-0.5}q^{0.67}$	Heat flux, reduced pressure	21.7
Gorenflo [15]	$h = h_0F_{PF}(q/q_0)^{n/}(R_p/R_{po})^{0.133}$, $h_0 = 4170$ (CO_2)	Heat flux, surface roughness	21.2
Lazarek and Black [16]	$Nu = 30Re^{0.857}Bo^{0.714}$, $Re = GD/\mu_l$	Boiling number/developed for small tubes	31.4
Tran et al. [17]	$h = 840(Bo^2We_l)^{0.3}(\rho_l/\rho_g)^{-0.4}$ kW/m^2K	Boiling number/developed for small tubes or channels	36.7
Liu and Winterton [6]	$h = ((Eh_{Dittus-Boelter})^2 + (Sh_{Cooper})^2)^{1/2}$	Including the Cooper model	25.6
Kattan et al. [18]	$h = ((0.0133Re_l^{0.69}Pr_l^{0.4}k_l/\delta)^3 + (0.023Re_v^{0.8}Pr_v^{0.4}k_v/D)^3)^{1/3}$ $Re_l = 4G(1-x)\delta/((1-\varepsilon)\mu_l)$, $Re_v = GxD/(\varepsilon\mu_v)$	Including effects of flow pattern	24.1

[a] Mean dev. $= \frac{1}{n}\sum_1^n ABS[((h_{pred} - h_{exp}) \times 100)/h_{exp}]$.

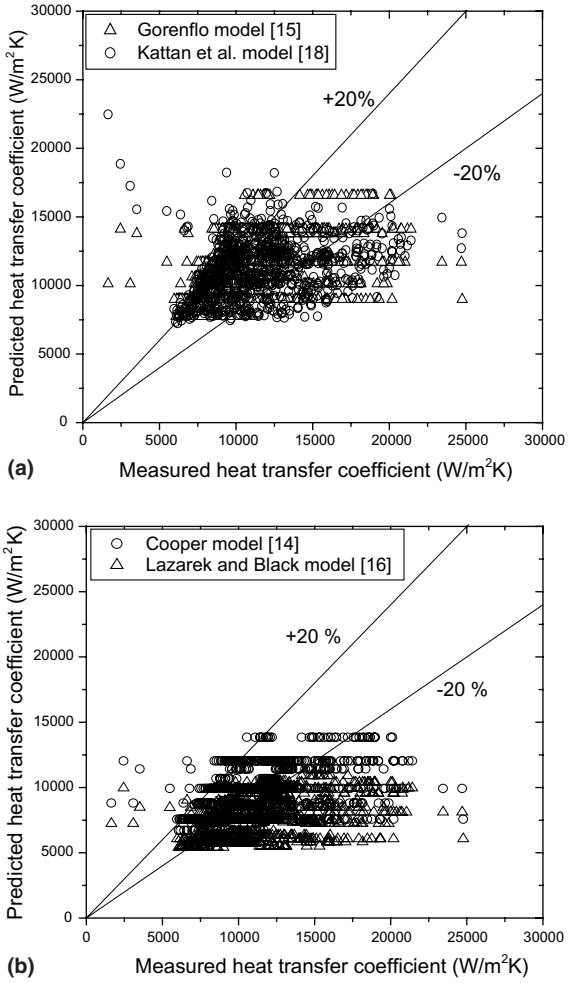

Fig. 9. Comparison of the present data with those of the existing models. (a) The Gorenflo model [15] and the Kanttan et al. model [18], (b) the Cooper model [14] and the Lazarek and Black model [16].

of CO_2 were much more significant than those of R134a. As the heat flux increases, the heat transfer coefficient becomes higher at all test conditions prior to dryout. Increasing the saturation temperature enhances the heat transfer coefficient by activating nucleate boiling heat transfer. As the mass flux increases, dryout becomes more pronounced due to an easier flow pattern transition and a larger liquid droplet entrainment. Decreasing of the hydraulic diameter of microchannels improves the heat transfer coefficient. The Cooper model [14] and the Gorenflo model [15], which were developed to predict nucleate boiling heat transfer coefficients, yield relatively good predictions of the present data with mean deviations of 21.7% and 21.2%, respectively.

Acknowledgments

This work was jointly supported by the Korea Science and Engineering Foundation (Grant no. R01-2002-000-00481-0), and the Carbon dioxide Reduction & Sequestration Center, one of the 21st Century Frontier R&D Programs in the Ministry of Science and Technology of Korea.

References

[1] J. Pettersen, Flow vaporization of CO_2 in microchannel tubes, Exp. Thermal Fluid Sci. 28 (2004) 111–121.
[2] Y. Zhao, M. Molki, M.M. Ohadi, S.V. Dessiatoun, Flow boiling of CO_2 in microchannels, ASHRAE Trans. 106 (1) (2000) 437–445.
[3] E. Hihara, S. Tanaka, Boiling heat transfer of carbon dioxide in horizontal tubes, in: Proceedings of 4th IIR-Gustav Lorentzen Conference, Purdue University, 2000, pp. 279–284.
[4] R.Yun, C.S. Choi, Y.C. Kim, Convective boiling heat transfer of carbon dioxide in horizontal small diameter tubes, in: Proceedings of 5th IIR-Gustav Lorentzen Conference, Guangzhou, China, 2002, pp. 298–308.
[5] Y. Zaho, M. Molki, M.M. Ohadi, Predicting flow boiling heat transfer of CO_2 in microchannel, in: Proceedings of ASME International Mechanical Engineering Congress and Exposition, New York, 2001.
[6] Z. Liu, R.H.S. Winterton, A general correlation for saturated and subcooled flow boiling in tubes and annuli, based on a nucleate pool boiling equation, Int. J. Heat Mass Transfer 34 (1991) 2759–2766.
[7] S.G. Kandlikar, Fundamental issues related to flow boiling in minichannels and microchannels, Exp. Thermal Fluid Sci. 26 (2002) 389–407.
[8] R.J. Maffat, Describing the uncertainties in experimental results, Exp. Thermal. Fluid Sci. 1 (1998) 3–17.
[9] R. Yun, Y. Kim, Flow regimes for horizontal two-phase flow of CO_2 in a heated narrow rectangular channel, Int. J. Multiphase Flow 30 (2004) 1259–1270.
[10] J. Pettersen, Flow Vaporization of CO_2 in Microchannel Tubes, Ph.D. Thesis, Norwegian University of Science and Technology, 2002.
[11] Z.Y. Bao, D.F. Fletcher, B.S. Haynes, Flow boiling heat transfer of R11 and HCFC123 in narrow passages, Int. J. Heat Mass Transfer 43 (2000) 3347–3358.
[12] W. Yu, D.M. France, M.W. Wambsganss, J.R. Hull, Two-phase pressure drop, boiling heat transfer, and critical heat flux to water in a small-diameter horizontal tube, Int. J. Multiphase Flow 28 (2002) 927–941.
[13] M.W. Wambsganss, J.A. Jendrzejczyk, D.M. France, Two-phase flow patterns and transitions in a small, horizontal, rectangular channel, Int. J. Multiphase Flow 17 (3) (1991) 327–342.
[14] M.G. Cooper, Heat flow rates in saturated nucleate pool boiling—a wide ranging examination using reduced properties, in: F. Thomas Irvine (Ed.), Advances in Heat Transfer, Academic Press, Orlando, 1984, pp. 157–239.

[15] D. Gorenflo, Pool boiling, in: VDI Gesellschaft Verfahrenstechnic und Chemieingenieurwesen (Ed.), English translation of VDI, Dsseldorf, 1993, pp. Ha 4–Ha 18.
[16] G.M. Lazarek, S.H. Black, Evaporative heat transfer, pressure drop and critical heat flux in a small vertical tube with R-113, Int. J. Heat Mass Transfer 25 (7) (1982) 945–960.
[17] T.N. Tran, M.W. Wambsganss, D.M. France, Boiling heat transfer with three fluids in small circular and rectangular channels, ANL-95/9, Illinois, 1995.
[18] N. Kattan, J.R. Thome, D. Favrat, Flow boiling in horizontal tubes: Part 3 Development of a new heat transfer model based on flow pattern, Trans. ASME J. Heat Transfer 120 (1998) 156–165.